

Als Manuskript gedruckt

Technische Universität Dresden
Herausgeber: Der Rektor

Optimal and Model Predictive Control of the Boussinesq Approximation

Part 1: Numerical implementation

Michael Hinze & Ulrich Matthes

MATH-NM-02-2004

Dezember 2004

Contents

1	Introduction	3
2	Mathematical model	4
2.1	Boussinesq approximation	4
2.1.1	Variational formulation	4
2.1.2	Existence and Uniqueness	5
2.2	Time discretization	5
3	Model predictive control	6
4	Numerical results	7
4.1	Introduction	7
4.2	Implementation and numerical examples	8
4.3	IC and Example 1	8
4.3.1	Control actions	9
4.3.2	Gradient scaling	9
4.3.3	Initial controls in steepest descent	12
4.3.4	Steepest descent step size	12
4.3.5	Time step	13
4.3.6	Simulation of practical control	15
4.3.7	Comparison of IC and optimal open loop control	15
4.3.8	Tracking of optimal control with IC	16
4.4	Model predictive control with $M > 1$	18
4.4.1	MPC and Example 1	18
4.4.2	MPC and Example 2	18
5	Discussion and Conclusions	19
6	Appendix	20

Optimal and Model Predictive Control of the Boussinesq Approximation

Part 1: Numerical implementation

Michael Hinze & Ulrich Matthes

Institut für Numerische Mathematik,

Technische Universität Dresden

D-01069 Dresden, Germany,

email: hinze@math.tu-dresden.de matthes@math.tu-dresden.de

Abstract

In this paper optimal and model predictive control applied to the Boussinesq approximation of the Navier-Stokes system is discussed. It focuses on mathematical modelling, discuss possible control scenarios, and provides a concise description of the numerical implementation. In a second part the associated numerical analysis will be presented.

1 Introduction

The Boussinesq approximation of the Navier-Stokes system is frequently used as mathematical model for fluid flow in semiconductor melts. In many crystal growth technics, such as Czochralski growth, and zone-melting technics the behavior of the flow has considerable impact on the crystal quality. It is therefore quite natural to establish flow conditions which guarantee desired crystal properties.

As a first step towards controlling the crystal-melt complex in Czochralski growth we study in the present paper optimal and model predictive control technics for the Boussinesq approximation. As control actions we consider distributed forcing, distributed heating, and boundary heating, as well as its combinations.

To the best of the authors knowledge up to now there are no contribution to model predictive control for the Boussinesq approximation. However, in the past decade considerable progress has been made in the field of flow control, see [5] for a comprehensive overview and further literature in the field. In the literature also contributions to optimal control of the Boussinesq approximation can be found. Here we mention the works [1] and [12].

The paper is organised as follows. In section 2 the variational form of the Boussinesq approximation is introduced and the time discretization scheme is presented. In section 3 model predictive control is introduced, and in section 4 numerical results are given. In section 5 we summarize the numerical results and give some conclusions.

2 Mathematical model

2.1 Boussinesq approximation

The Boussinesq approximation of the Navier-Stokes system in the primitive setting is given by

$$(1) \quad \begin{aligned} \frac{\partial y}{\partial t} - \nu \Delta y + \nabla p &= -(y \nabla) y - \gamma g \tau + u_F && \text{in } Q \\ -\operatorname{div} y &= 0 && \text{in } Q \\ y &= 0 && \text{on } \Sigma \\ y(0) &= y_0 && \text{in } \Omega \\ \frac{\partial \tau}{\partial t} - a \Delta \tau &= -(y \nabla) \tau + u_Q && \text{in } Q \\ a \partial_\eta \tau &= \alpha(u - \tau) && \text{on } \Sigma \\ \tau(0) &= \tau_0 && \text{in } \Omega \end{aligned}$$

were y, p, τ denote the velocity, pressure and temperature field, respectively. Further a denotes the thermal diffusivity, ν the kinematic viscosity, $g \in \mathbf{R}^2$ the acceleration of gravity, γ the coefficient of volume expansion, and α a positive number. Here $\Omega \subset \mathbf{R}^2$ denotes an open, bounded domain, with boundary $\Gamma = \partial\Omega$ which is assumed to be sufficiently smooth. We set $Q := (0, T) \times \Omega$ and $\Sigma := (0, T) \times \Gamma$ with T denoting the time horizon.

The variables u, u_F, u_Q denote the control actions; u the boundary temperature, u_F distributed force, and u_Q distributed heating.

To prepare for the variational formulation of (1) we further introduce the solenoidal spaces $H = \{v \in C_0^\infty(\Omega)^2 : \operatorname{div} v = 0\}^{-\|\cdot\|_{L^2(\Omega)^2}}$ and $V = \{v \in C_0^\infty(\Omega)^2 : \operatorname{div} v = 0\}^{-\|\cdot\|_{H^1(\Omega)^2}}$.

Also if X is a Banach space, $L^p(0, T; X)$ denotes the space of L^p -integrable functions from $(0, T)$ into X , which itself is a Banach space.

2.1.1 Variational formulation

Following [1] and [15], the variational formulation of (1) reads: Given $f = (u_F, u_Q)^T \in L^2(0, T; V^* \times H^1(\Omega)^*)$, $u \in L^2(0, T; L^2(\Gamma))$ and $Y_0 \in H \times L^2(\Omega)$, find $Y \in L^2(0, T; V \times H^1(\Omega))$ satisfying

$$\begin{aligned} \frac{d}{dt}(Y, U) + a(Y, U) + b(y, Y, U) + (\gamma g \tau, v)_{L^2(\Omega)^2} + (\alpha \tau, \eta)_{L^2(\Gamma)} = \\ (2) \quad (f, U)_{(V \times H^1(\Omega))^* \times (V \times H^1(\Omega))} + (\alpha u, \eta)_{L^2(\Gamma)} \quad \forall U \in V \times H^1(\Omega), \text{ and almost all } t \in (0, T), \end{aligned}$$

and

$$(3) \quad Y(0) = Y_0 := \begin{pmatrix} y(0) \\ \tau(0) \end{pmatrix}.$$

Here we use the notation

$$Y := \begin{pmatrix} y \\ \tau \end{pmatrix}, \quad U := \begin{pmatrix} v \\ \eta \end{pmatrix}, \quad W := \begin{pmatrix} w \\ \kappa \end{pmatrix},$$

and forms $a(\cdot, \cdot)$ and $b(\cdot, \cdot, \cdot)$ are defined by

$$\begin{aligned} a(Y, U) &:= \nu \int_{\Omega} \nabla y \nabla u \, dx + a \int_{\Omega} \nabla \tau \nabla \eta \, dx \quad \forall Y, U \in V, \\ b(U, Y, W) &:= \int_{\Omega} (v \nabla) y w \, dx + \int_{\Omega} (v \nabla) \tau \kappa \, dx \quad \forall U, Y, W \in V \times H^1(\Omega), \end{aligned}$$

and

$$(\alpha \tau, \cdot) := (S(\alpha \tau), S \cdot)_{L^2(\Gamma)} \in V^* \text{ with } S \text{ denoting the trace operator.}$$

2.1.2 Existence and Uniqueness

Analogously to [15, Chap. III §3] we can prove existence and uniqueness of solutions to (2)-(3).

Theorem 2.1. *Let $u_F \in L^2(0, T; V^*)$, $u_Q \in L^2(0, T, H^1(\Omega)^*)$, $u \in L^2(0, T; L^2(\Gamma))$ and $y_0 \in H$, $\tau_0 \in L^2(\Omega)$. Then there exists a unique solution Y of (2)-(3) which satisfies $Y \in L^2(0, T; V \times H^1(\Omega))$, $Y' \in L^2(0, T; V^* \times H^1(\Omega)^*)$. Moreover, $Y \in C([0, T]; H \times L^2(\Omega))$ and*

$$(4) \quad Y(t) \rightarrow Y_0, \text{ in } H \times L^2(\Omega), \text{ as } t \rightarrow 0.$$

For the convenience of the reader a proof of this theorem is provided in the Appendix 6.

2.2 Time discretization

As time discretization scheme for (1) we use a semi-implicit Euler with time step size dt . Semi implicit here means that the convective parts are discretized explicitly.

Giving y^i, τ^i the resulting system for y^{i+1} and τ^{i+1} at time instance t_{i+1} in the primitive setting reads:

$$(5) \quad \frac{y^{i+1} - y^i}{dt} - \nu \Delta y^{i+1} + \nabla p^{i+1} = -(y^i \nabla) y^i - \tau^{i+1} \gamma g + u_F^{i+1} \quad \text{in } \Omega,$$

$$(6) \quad -\operatorname{div} y^{i+1} = 0 \quad \text{in } \Omega,$$

$$(7) \quad y^{i+1} = 0 \quad \text{on } \Gamma,$$

$$(8) \quad \frac{\tau^{i+1} - \tau^i}{dt} - a \Delta \tau^{i+1} = -(y^i \nabla) \tau^i + u_Q^{i+1} \quad \text{in } \Omega,$$

$$(9) \quad a \partial_{\eta} \tau^{i+1} = \alpha (u^{i+1} - \tau^{i+1}) \quad \text{on } \Gamma,$$

where $y^0 := y_0$ and $\tau^0 = \tau_0$ with y_0, τ_0 from (1).

The treatment of the convection term in (8) allows to compute the temperature τ^{i+1} by solving (8),(9), and subsequently the velocity y^{i+1} and p^{i+1} by (5)-(7). To anticipate the discussion, this coupling is also advantageous for the evaluation of descent directions in the formulation of the instantaneous control method.

It is worth noting that for given $y^i, \tau^i, u_F^{i+1}, u_Q^{i+1}, u^{i+1}$ in $V \times H^1(\Omega) \times V^* \times (H^1)^* \times L^2(\Gamma)$ the system (5)-(9) admits a unique weak solution $y^{i+1} \in V, \tau^{i+1} \in H^1(\Omega)$, compare [3].

3 Model predictive control

For an integer $M \geq 1$ given, model predictive control, frequently also called receding horizon control, applies repeatedly optimal control on a finite discrete time horizon containing M time steps, and uses the optimal control action associated to the first time step to steer the system towards a prescribed desired state $(z, S) = (z(t, x), S(t, z))$. In the present work the optimization problem associated to time step i is given by:

$$(10) \quad \min J(y, \tau, u, u_F, u_Q) = \sum_{j=i+1}^{i+M} \left(\frac{c_0}{2} \int_{\Omega} (y^j - z^j)^2 dx + \frac{c_1}{2} \int_{\Omega} (\tau^j - S^j)^2 dx \right. \\ \left. + \frac{c_2}{2} \int_{\Gamma} u^j{}^2 dx + \frac{c_3}{2} \int_{\Omega} u_F^j{}^2 dx + \frac{c_4}{2} \int_{\Omega} u_Q^j{}^2 dx \right)$$

for $(y, \tau, u, u_F, u_Q) \in V^M \times H^1(\Omega)^M \times L^2(\Gamma)^M \times H^M \times (L^2)^M$, subject to:

$$(11) \quad \begin{aligned} \tau^{j+1} - dt a \Delta \tau^{j+1} &= dt c_Q u_Q^{j+1} + \tau^j - dt (y^j \nabla) \tau^j && \text{in } \Omega \\ a \partial_{\eta} \tau^{j+1} &= \alpha (u^{j+1} - \tau^{j+1}) && \text{on } \Gamma \\ y^{j+1} - dt \nu \Delta y^{j+1} + \nabla (dt p^{j+1}) &= -dt \gamma g \tau^{j+1} + dt c_F u_F^{j+1} + y^j - dt (y^j \nabla) y^j && \text{in } \Omega \\ -\text{div } y^{j+1} &= 0 && \text{in } \Omega \\ y^{j+1} &= 0 && \text{on } \Gamma \end{aligned}$$

with $j = i, \dots, i + M - 1$. In particular in this setting we assume that controls are at least square integrable functions.

Since the transition constraints (11) for given u_Q, u_F, u admit an unique solution, we may introduce the reduced functional

$$\hat{J}(u, u_F, u_Q) := J(y(u, u_F, u_Q), \tau(u, u_f, u_Q), u, u_F, u_Q).$$

Problem (10),(11) then is equivalent to

$$(12) \quad \min \hat{J}(u, u_F, u_Q), \quad \text{for } (u, u_F, u_Q) \in L^2(\Gamma)^M \times H^M \times (L^2)^M.$$

Since \hat{J} is a quadratic functional and the constraints (11) are linear, problem (12) admits a unique solution.

It is well known, that the gradient $\hat{J}'(u, u_F, u_Q)$ can be expressed with the help of the adjoint variables associated to (10),(11). Let us discuss the details for the case $M = 1$ which also forms the starting point of our investigations of the instantaneous control strategy. In the following, superscripts are dropped. The adjoint equations associated to problem (11) for $M = 1$ are given by

$$\begin{aligned} p^y - dt \nu \Delta p^y + \nabla p^p &= c_0 (y - z) && \text{in } \Omega, \\ p^y &= 0 && \text{on } \Gamma, \\ -\text{div } p^y &= 0 && \text{in } \Omega, \\ p^{\tau} - dt a \Delta p^{\tau} &= c_1 (\tau - S) - dt \gamma g p^y && \text{in } \Omega, \\ a \partial_{\eta} p^{\tau} &= -\alpha p^{\tau} && \text{on } \Gamma, \end{aligned}$$

where p^y, p^p denote the adjoint velocity field and pressure, respectively, and p^τ the adjoint temperature field. With the adjoint variables available, there holds

$$(13) \quad \begin{aligned} \left(\hat{J}'(u, u_F, u_Q), (v, v_f, v_Q) \right) &= (c_2 u - dt a \partial_\eta p^\tau, v)_{L^2(\Gamma)^2} \\ &+ (c_3 u_F + dt p^y, v_F)_H + (c_4 u_Q + dt p^\tau, v_Q)_{L^2} \end{aligned}$$

In the instantaneous control approach the reduced optimization problem (12) is solved approximately, by applying only one steepest descent step to obtain an approximate solution [2, 7, 8, 9, 10, 11, 13, 16]. Instantaneous control therefore may be regarded as an inexact variant of MPC for $M = 1$.

To compute the gradient $\hat{J}'(u, u_F, u_Q)$ for given u, u_F, u_Q the coupled system of equations (11) and (13) has to be solved for p^y, p^p, p^τ . This is accomplished by using a preconditioned conjugate steepest descent method for the associated Schur-complement as proposed in [4] and [6], say.

In system (1) different control actions are possible. To optimize all of them simultaneously a suitable scaling of the gradient $\hat{J}'(u, u_F, u_Q)$ in the steepest descent method has to be introduced. This may be regarded as preconditioning and is achieved by replacing \hat{J}' by $D\hat{J}'$ with D denoting as suitable 3×3 diagonal matrix. For more details see section 4.3.2. The step size in the steepest descent method for \hat{J} is computed exactly for the instantaneous control (IC) method. This is possible since \hat{J} is quadratic in its arguments u, u_F and u_Q , compare [6]. The optimal step size in direction d is computed via a steepest descent step with trial step size ρ_p and calculating the minimum of the parabola defined by $\hat{J}(u_*)$, $\hat{J}'(u_*)$ and $\hat{J}(u_* + \rho_p d)$, where $u_* = (u, u_F, u_Q)^T$. For more details we also refer to section 4.3.4.

4 Numerical results

4.1 Introduction

We test IC and MPC for two numerical examples. The control goal in both examples consists in tracking of a desired velocity and a desired temperature field. In example 1 the desired (normalized) temperature is zero and the desired velocity field is obtained from a forward simulations with pre-specified boundary temperature, see section 4.3 for details. We investigate the performance of IC for all three control actions. It turns out that IC performs very well. These control results can be improved by applying MPC to larger time horizons, i.e. for $M > 1$. This is illustrated for boundary control in section 4.4.1. In example 2 the desired velocity field is zero, and a non-trivial temperature field should be tracked. The control action here is given by boundary control alone. IC fails but MPC is able to track the desired states see section 4.4.2.

In example 2 a zero velocity field but different temperatures are desired. The control aim is to find a good trade-off between reaching the two aims in the case of boundary control. The difficulty are the different time scales of steering the temperature vs. velocity field. The IC fails, see 4.4.2, but the MPC is able to compute an acceptable control.

Parameter	Example 1	Example 2
c_0	$2 \cdot 10^6$	$2 \cdot 10^6$
c_1	2	20
c_2	$2 \cdot 10^{-4}$	$2 \cdot 10^{-3}$
c_3	$2 \cdot 10^{-2} dt$	$2 \cdot 10^{-3} dt$
c_4	$2 \cdot 10^{-2} dt$	$2 \cdot 10^{-3} dt$
a	$1.44 \cdot 10^{-4}$	$1.44 \cdot 10^{-3}$
ν	$2.5 \cdot 10^{-4}$	$1 \cdot 10^{-3}$
γ	$2.1 \cdot 10^{-4}$	$2.1 \cdot 10^{-4}$
g	$(0, -9.81)$	$(0, -9.81)$

Table 1: Parameters for the examples 1 (left), and 2.

4.2 Implementation and numerical examples

All numerical examples are computed on a 20×20 equidistant grid on $\Omega := (0, 1)^2$. For the velocity-pressure discretization the related staggered grid is used. The temperature is taken on the pressure nodes. The discretization of the Laplacian is based on the 5-point star. The parameters in our computations can be found in table 1. The resulting Reynolds-number for example 1 is $Re = \frac{L \|z\|}{\nu} = 33.2$ (with $L = 1$ unit square), and for example 2 it depends on the control. The Grashof-number for example 2 is $Gr = \frac{\gamma |g| L^3 (\delta S)}{\nu^3} = 2060$ (were δS denotes the maximal temperature difference in the desired temperature field S) and for example 1 it depends on the control.

All elliptic subproblems are solved with the SSOR method, which for the numerical examples presented below converges within a few steps.

For the parameter α in the boundary condition we also choose $\alpha = \infty$ i.e. Dirichlet conditions, to test the robustness of the algorithm.

The boundary conditions are $y = 0$ on Γ , and $\tau = 0$ on Γ if no boundary temperature control is used. The initial conditions are chosen as $y_0 \equiv 0$ and $\tau_0 \equiv 0$.

The time horizon for the integrations of J is given by $[0, T]$, with $T = 360$.

4.3 IC and Example 1

In this example we present a detailed discussion of the instantaneous control strategy (IC), which proves very powerful in various applications to flow control, see [2, 6] and the literature cited there. IC is an inexact variant of MPC for $M = 1$. For the approximate solution of the optimality system in this case only one steepest descent step is applied. The parameters used in our computations for this case can be found in table 1, left.

The desired state z for example 1 is depicted in figure 1, left. It is the stationary velocity field obtained after a time of $t = 10000$ by choosing the constant boundary temperature of 1 on the right half of the lower boundary, and 0 otherwise. All parameters for this simulation are the same as in example 1.

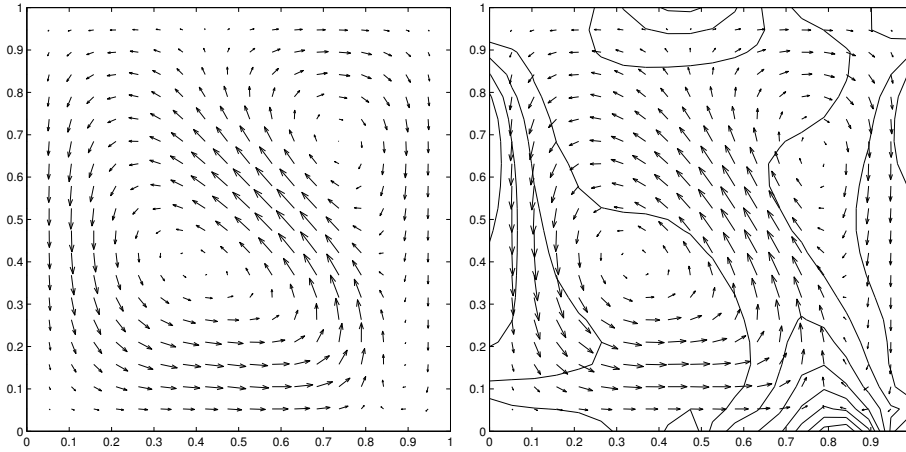


Figure 1: left: desired state, right: flow controlled by boundary temperature

As desired temperature $S \equiv 0$ is chosen but with only a small weight in the cost functional, see table 1. For tracking of an optimal trajectory (see 4.3.8) the desired state is the solution of an optimal control problem. For further details and results see [14].

4.3.1 Control actions

Three different control actions are investigated: distributed force, distributed heat, boundary temperature, and also their combinations. In all cases the steepest descent step for IC is initialized with zero control. The optimal steepest descent step size is used and the time step is set to $dt = 0.8$. The results are shown in the figure 1, right, and figures 2, 3, 4. This figures show the temperature and velocity field at $T = 360$. In all cases the IC performs very well and is able to reach the desired state approximately. The evolution of cost functional J is shown in figure 5. We take up again the case of boundary temperature control in section 4.4.1.

4.3.2 Gradient scaling

Gradient scaling is preconditioning of the steepest descent method. It needs to be applied if combinations of control actions are used. In figure 6 the values of the time integrated cost functional are presented for the parameter range $c_F, c_Q \in [10^{-7}, 10^{-1}] \times [10^{-5}, 10]$. as expected for this example small values of c_Q give the best reduction of the cost functional. Here we apply diagonal scaling with the diagonal matrix

$$D = \begin{pmatrix} 1 & 0 & 0 \\ 0 & c_F & 0 \\ 0 & 0 & c_Q \end{pmatrix}.$$

In all examples presented we set $c_F = 10^{-3}, c_Q = 0.3$. (All except in this subsection investigating the parameter space for Example 1.) For this choice of parameters IC also

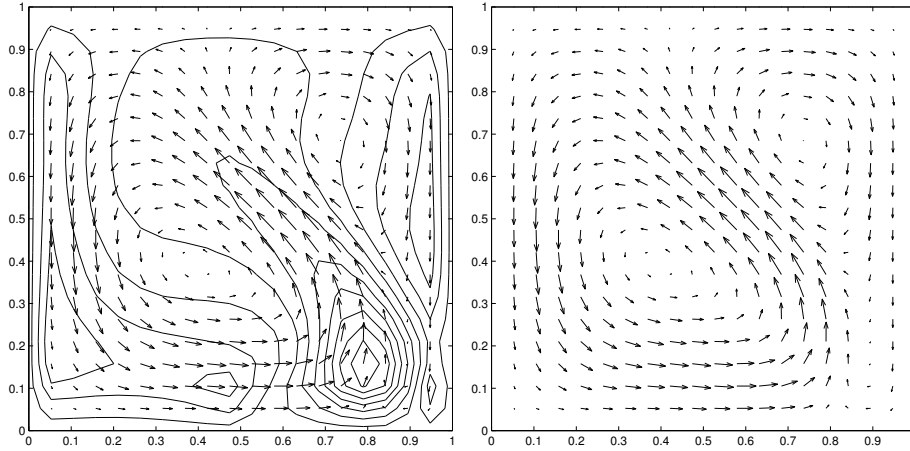


Figure 2: left: flow controlled by distributed heat, right: flow controlled by distributed force

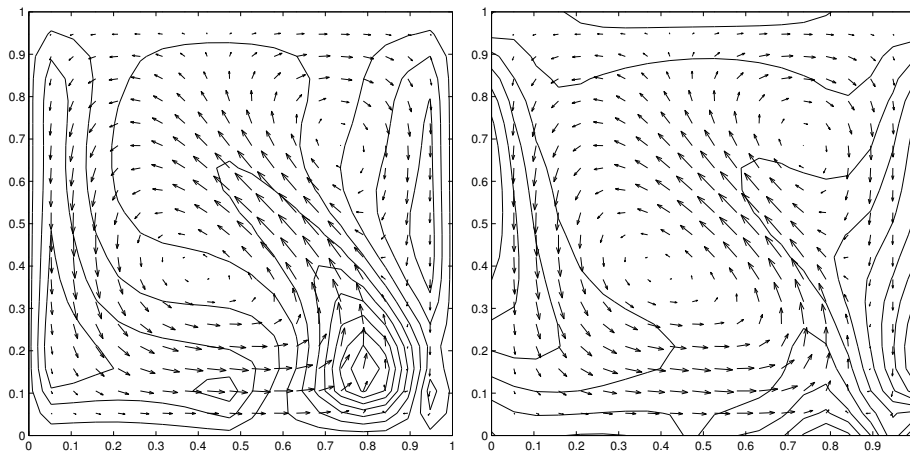


Figure 3: left: flow controlled by boundary temperature and distributed heat , right: flow controlled by boundary temperature and distributed force

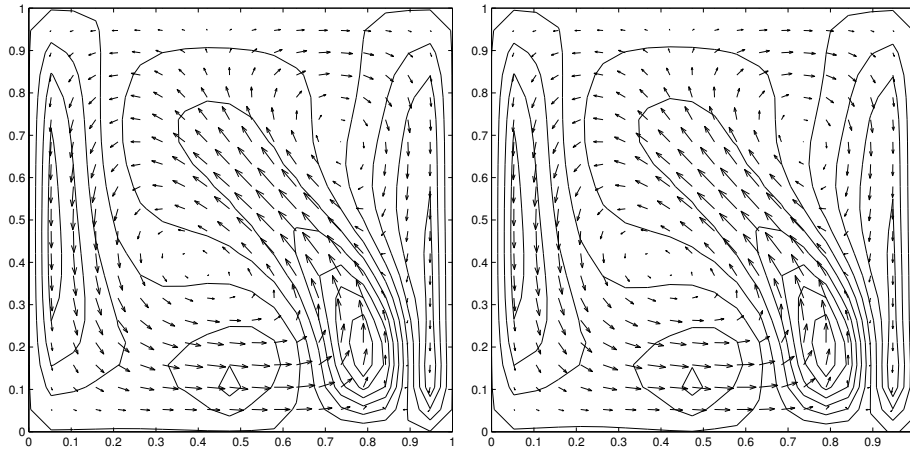


Figure 4: left: flow controlled by distributed heat and distributed force, right: flow controlled by all three controls

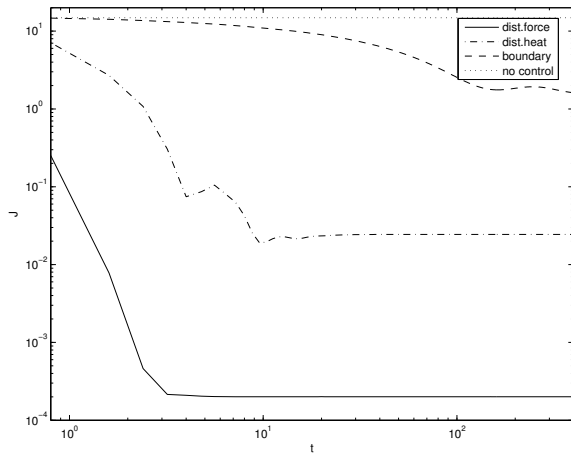


Figure 5: Evolution of cost functional J for some differed control actions.

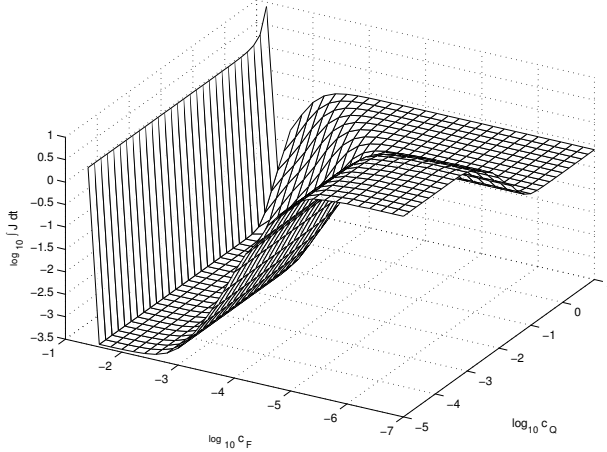


Figure 6: different scaling of controls, all controls,

performs very well in the example of [14]. However, we note no general rule for choosing the parameters c_F, c_Q is known yet.

4.3.3 Initial controls in steepest descent

As initial values for the steepest descent method either the zero control or the control from the optimization at the previous time slice are chosen. It is observed that choosing zero control as initialization the performance of MPC/IC is very sensitive with regard to gradient scaling.

It is remarkable, that IC initialized with the control of the previous time slice in the long run performs similar to MPC with $M = 1$, provided the controls vary not too much between the time slices.

Start with zero control is worse in cases where combinations of controls are used. On the other hand using the control from the previous time slice sometimes turns out to be less robust. This strongly depends on the dynamical behavior of the underlying physical process, see [14] for details.

4.3.4 Steepest descent step size

Since the IC control problem (10),(11) is linear-quadratic the optimal step size ρ^* in the steepest descent algorithm can be calculated exactly. In the calculations presented the value ρ^* is taken as minimum of the scalar parabola $h(\rho)$ defined by the function values $\hat{J}(u), \hat{J}(u + \rho_p d)$ and the derivative $\hat{J}'(u)d$, where $d := -J'(u)$ and ρ_p is an estimation of the steepest descent step size taken from the optimization problem at the previous time slice. Compared to taking constant steepest descent step sizes the numerical overhead is caused by an additional function evaluation $\hat{J}(u + \rho_p d)$, which amounts to solving (11) with control $u + \rho_p d$.

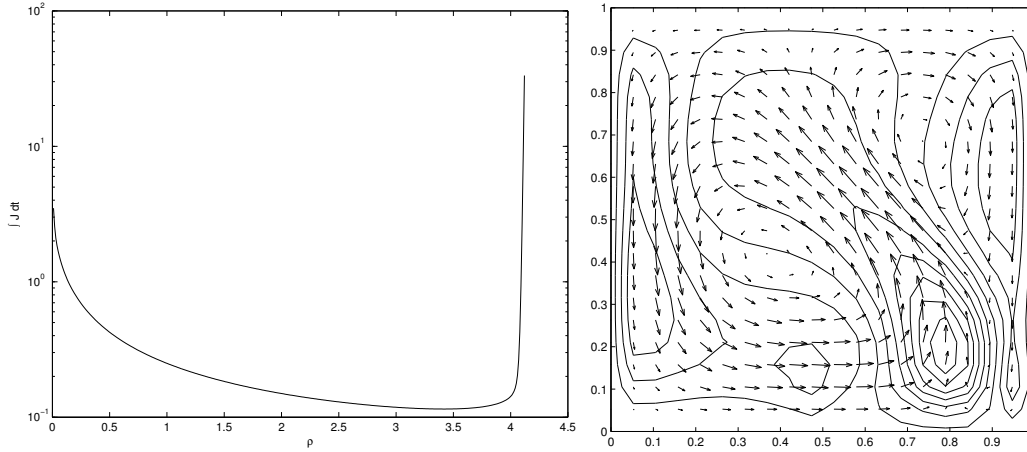


Figure 7: left: distributed heat, integrated functional for different constant steepest descent step sizes, right: distributed heat, $dt = 0.1$

Using a constant steepest descent step size ρ results in a slightly faster algorithm but requires knowledge about the magnitude of this step size. If the step size is too large the method diverges. Too short steepest descent steps lead to ineffective controls, in particular when using zero initial control. In figure 7, left, the dependence of $\int J dt$ on ρ is shown. Short steepest descent steps are worse with regard to reducing the functional J . On the other hand, if the steepest descent step is too large, the steepest descent method diverges. Because a useful steepest descent step size is not known a priori, we suggest to use the optimized steepest descent step size instead of a fixed steepest descent step.

4.3.5 Time step

The quality of controls obtained by the IC method depends on the length of the time step. Small time steps cause only weak control actions, so that time steps as large as possible, obeying the CFL conditions, should be taken. At greater time steps the control is more effective and so the IC predicts a greater win from producing stronger forces and heatings.

So the time step for reasons of control effectivity and computing time should be made as large as possible.

Now the performance of control at different time steps is investigated. For distributed heating compare the flows together with the temperature field in figure 7, right $dt = 0.1$, figure 2, left $dt = 0.8$, and figure 8 $dt = 6.4$ respectively. As one can see flows and temperature distributions in all three cases look very similar. For larger time steps the controls and states are oscillating between two states, which are depicted in figure 8. We note, that this is a purely numerical behavior caused by the large time step chosen.

The dependence of $\int J dt$ of dt is shown in figure 9, left. As one can see cost reduction is most effective for $dt \approx 1.1$.

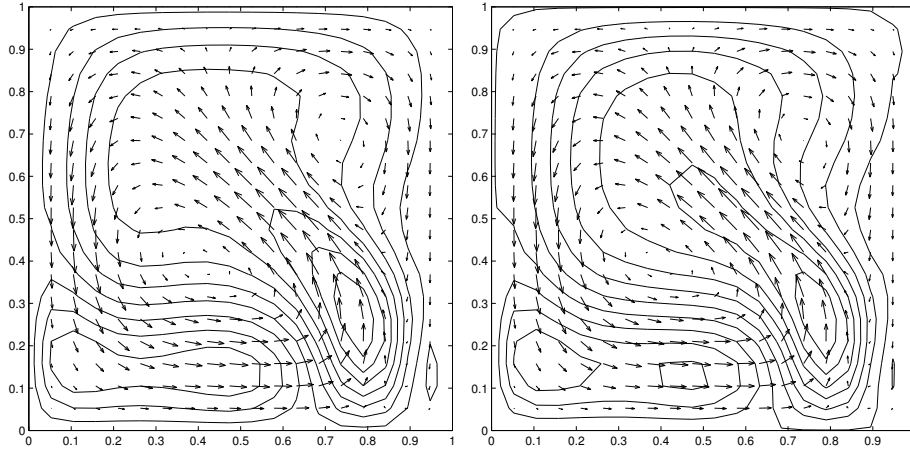


Figure 8: distributed heat, $dt = 6.4$, the state and control are oscillating between this two states

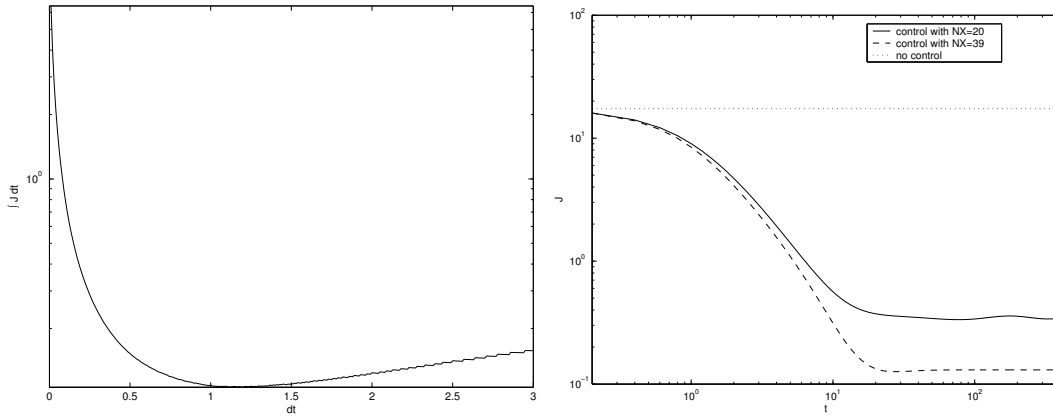


Figure 9: left: distributed heat and boundary temperature for different time steps dt , right: distributed heat. The control from the coarser grid also works well on the finer grid.

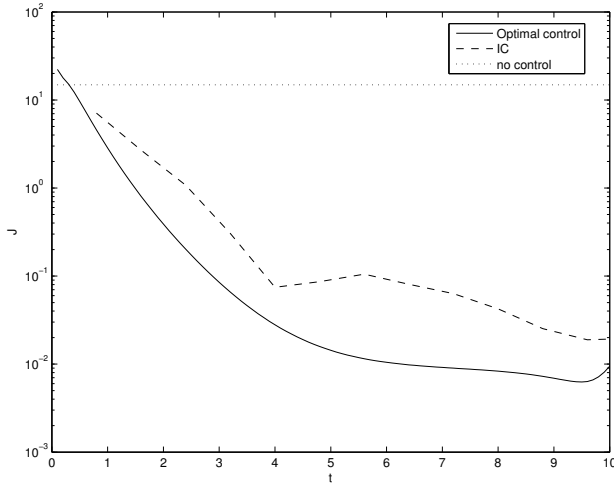


Figure 10: instantaneous control vs. optimal control

4.3.6 Simulation of practical control

In order to check the liability of numerically computed control procedures, the controls calculated on a 20×20 grid are applied to a discrete problem on a 39×39 grid. To extend the control, linear interpolation is used.

As figure 9, right shows, instantaneous controls obtained on the coarse grid perform pretty well also on the finer grid.

4.3.7 Comparison of IC and optimal open loop control

We now compare IC to optimal open loop control (OC). To obtain a discrete in time optimal open loop control on the time horizon $[0, T]$ the latter is divided into M time slices, and the cost functional

$$\begin{aligned}
 J_{OC}(y, \tau, u, u_F, u_Q) &= \sum_{i=1}^M \left(\frac{c_0}{2} \int_{\Omega} (y^i - z)^2 dx + \frac{c_1}{2} \int_{\Omega} (\tau^i - S)^2 dx \right. \\
 (14) \quad &\quad \left. + \frac{c_2}{2} \int_{\Gamma} (u^i)^2 dx + \frac{c_3}{2} \int_{\Omega} (u_F^i)^2 dx + \frac{c_4}{2} \int_{\Omega} (u_Q^i)^2 dx \right)
 \end{aligned}$$

is minimized s. t. the constraints (5)-(9), i.e. we solve (10),(11) on $[0, T]$. Numerically this is performed by applying a limited memory BFGS method on the fully discrete system. We note that the discrete optimization problem contains $3 \cdot 10^5$ unknowns. The evolution of the cost functional (at each time slice) is compared to that obtained by IC in figure 10. The control mechanism in this case is distributed heating. Parameters taken are $M = 100$ and $dt = 0.1$ for OC. For IC $dt = 0.8$ is chosen because shorter time horizons are worse, see 4.3.5. The coefficients and desired states are that of example 1, compare section 4.2.

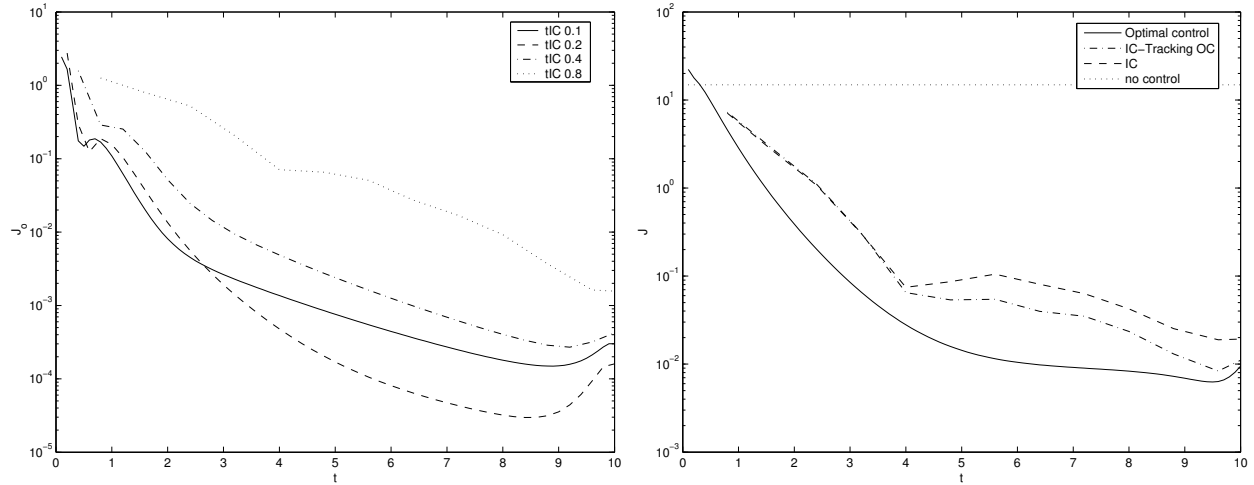


Figure 11: tracking of optimal control with IC: evolution of J_o for tracking of optimal state (left), and comparison of J of optimal control, IC for tracking of the optimal state, and IC applied to tracking of the desired state of the optimal control problem with $dt = 0.8$ (right).

4.3.8 Tracking of optimal control with IC

Once an optimal open loop trajectory is known it may serve as dynamical desired state to be tracked by the MPC strategy. In this context MPC, and in particular IC, serve as (nonlinear) closed loop control mechanisms. In figure 11 the results for IC and varying time step sizes dt are shown, where the control mechanism is distributed heating. As can be seen, IC is able to track the optimal open loop trajectory.

We note that for IC tracking the optimal trajectory and IC applied to original desired state the cost functionals are different. In the case of IC tracking the optimal trajectory, the functional is

$$J_o(t) = \frac{c_0}{2} \int_{\Omega} (y(t) - y(t)^*)^2 dt + \frac{c_1}{2} \int_{\Omega} (\tau(t) - \tau(t)^*)^2 dt + \dots$$

where $(y(t)^*, \tau(t)^*)$ denotes the optimal state. The original cost functional is given by

$$J(t) = \frac{c_0}{2} \int_{\Omega} (y(t) - z)^2 dt + \frac{c_1}{2} \int_{\Omega} (\tau(t) - S)^2 dt + \dots$$

In figure 11, left, the evolution of J_o for tracking the optimal control for different time steps, is shown. The method works very well, especially for $dt = 0.1$ and $dt = 0.2$. In figure 11, right the same is shown now J for the difference to the desired state of the original problem. Note that J is also calculated for IC tracking the optimal trajectory (which cost functional is in fact J_o). The dashed line represents the evolution of J for IC applied to track the desired state of the optimal control problem. The dash-dotted line shows the evolution of J for tracking of the optimal trajectory y^*, τ^* obtained from the optimal control problem. The solid line shows the evolution of J for the optimal control.

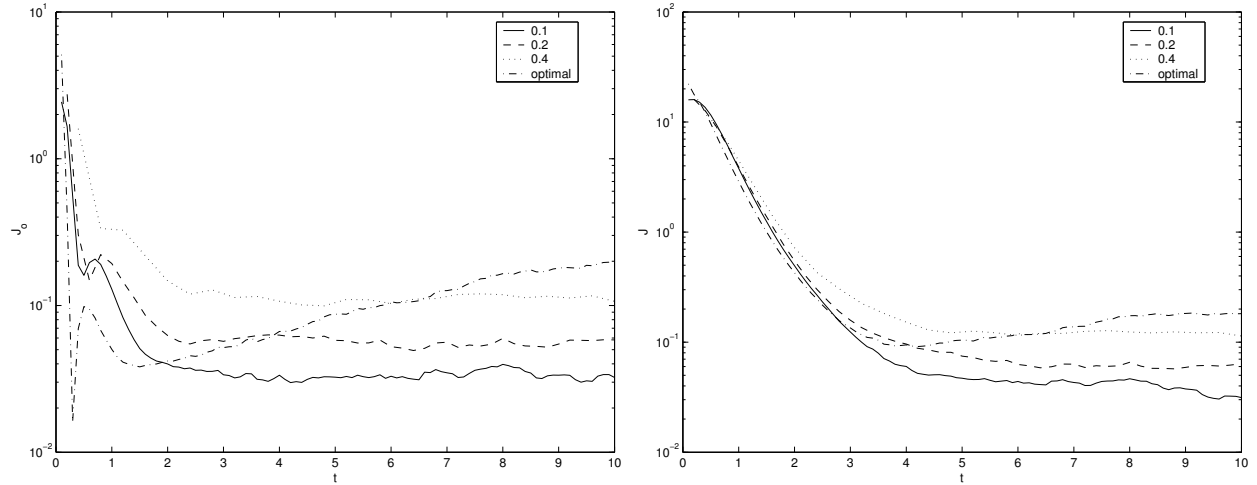


Figure 12: tracking of optimal control with IC including perturbations; evolution of J for tracking of optimal state (left), and comparison of optimal control and IC tracking the optimal state (right)

For IC is $dt = 0.8$ in both cases. Note that, as shown in the figure 11, right, IC tracking the optimal trajectory would even better with shorter time steps (contrary to IC applied to the original problem). As one can see IC in this example is well suited to track optimal trajectories (in the sense of a nonlinear closed loop controller) and also provides suboptimal controls with cost of the same magnitude as those of the optimal control procedure.

To investigate whether IC is able to stabilize a disturbed system random disturbances β are added at each time instance;

$$u_F^{dis} = u_F + \beta_F, \quad u_Q^{dis} = u_Q + \beta_Q$$

The functions β_F, β_Q are random numbers defined in the corresponding nodes equally distributed over $[-1, 1]$. To get an impression of the size of the disturbances we mention that their size is approximately 17 times that of the control action in the undisturbed case after the initial decrease.

Figure 12 shows the same quantities as figure 11, but for the disturbed case. In the left figure the J is the cost functional of IC with $z(t) = y^*(t), S(t) = \tau^*(t)$, where y^*, τ^* denote the optimal state. In the right figure the J is also the cost functional of IC but z and S are the same as for the optimal control.

As one can see, IC is able to track the perturbed optimal trajectory in the sense of a closed-loop controller, whereas the unperturbed optimal control strategy seems to fail.

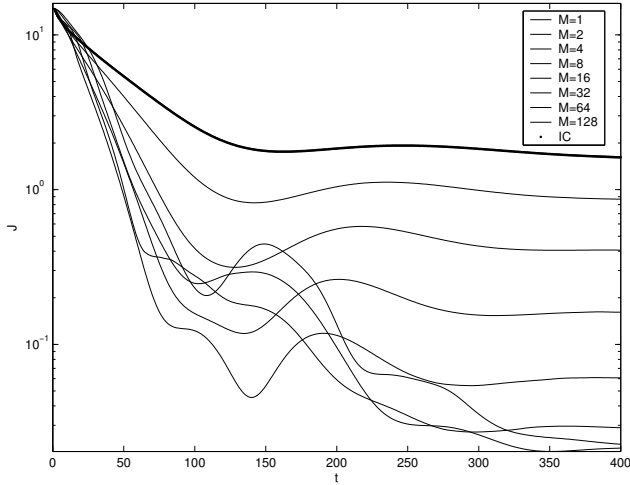


Figure 13: Performance of MPC in example 1, start with control from last time slice

4.4 Model predictive control with $M > 1$

4.4.1 MPC and Example 1

Now we try to improve the boundary temperature control by using MPC. As in the case of IC, we only use one steepest descent step to solve the corresponding optimization problems approximately. The results are presented in figure 13. To compare the performance of MPC to that of IC only the values of the first addend in 10 are shown. Their values compare to those of the cost functional used for IC. As a result MPC with $M = 16, \dots, 64$ and boundary heating reduces the (instantaneous) cost functional slower but in the long run as good as distributed heating with IC, see figure 5 and subsection 4.3. This is a substantial improvement to the control with IC.

4.4.2 MPC and Example 2

IC is not always successful in steering system states to desired states. However, as will be presented in the following, MPC on larger time horizons in general achieves this goal instead. In the present example we choose $z \equiv 0$, and the desired temperature distribution is given by

$$S := \begin{cases} 1 & \text{in } [0.5, 1) \times (0, 1) \\ 0 & \text{in } (0, 0.5) \times (0, 1). \end{cases}$$

As control action boundary control is chosen. This means that the control problem consists in establishing different temperatures in the left and the right part of the domain, respectively, with velocity as small as possible. The parameters of the computation are shown in table 1, right. We investigate (10),(11) for varying M , i.e. we vary the length of the prediction horizon in MPC.

As figure 14 shows, MPC with $M \geq 8$ has to be applied in order to reduce the value of the cost functional. Smaller prediction horizons do not yield a reduction which is mainly

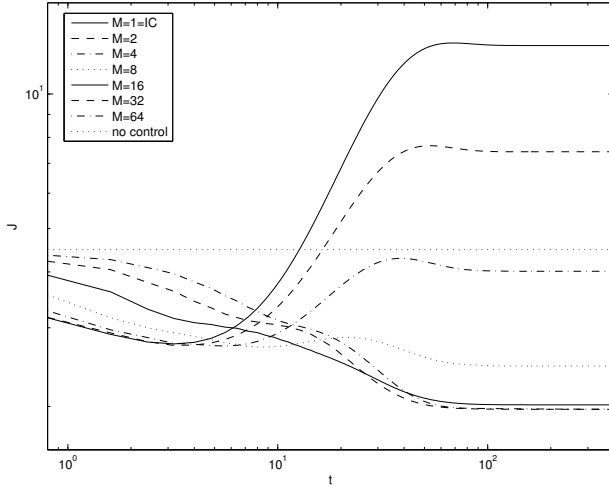


Figure 14: Performance of MPC in example 2

caused by the fact that the velocity only has a negligible influence on the gradient of the cost functional for small time horizons. We also note that in this case the increase of $|y - z|$ is superior over the decrease of $|\tau - S|$.

5 Discussion and Conclusions

Several control approaches to the Boussinesq approximation of the Navier-Stokes system are presented. Against the background of real-time control the instantaneous control method (IC) and model predictive control (MPC) mechanisms are studied in detail. As control actions, volume forces, distributed and boundary heating are considered.

IC performs very well in most of the investigated scenarios. Concerning the use of the control actions we may propose the following recipes;

- If tracking of a velocity is the control goal, either volume forces, or distributed heating, or a combination of both should be applied. Compared to their performance boundary temperature is less effective.
- If tracking of temperature distributions is the control goal, distributed heating combined with boundary heating should be applied. The influence of volume forces in this case is negligible.
- If a combination of control actions is chosen, the gradient of the cost functional has to be appropriately preconditioned in order to obtain a successful control method.

As is pointed out in section 4.4.2, especially for tracking of temperature distributions, MPC on sufficiently large time horizons has to be applied.

IC also presents a powerful tool in the context of nonlinear closed-loop control. If an open-loop optimal control strategy for a process is given (i.e. computed a priori), IC may

be used as a fast closed loop control mechanism which is capable of tracking the optimal open-loop control strategy, even in the presence of perturbations.

It is astonishing how well IC, and MPC perform in the sense of suboptimal control strategies for optimal control problems, as figures 10-12 indicate. These technics therefore also offer promising control tools for more realistic and complex configurations as they are dealt with in crystal growth, say.

6 Appendix

Proof of existence and uniqueness

Subsequently we use the notation $U = (v, \eta), Y = (y, \tau), W = (w, \kappa)$, and c denotes a positive generic constant. Similar to [15, Lemma 3.4]. we have

Lemma 6.1. *There holds*

$$|b(U, Y, W)| \leq c |v|_{L^2} \|Y\|_{V \times H^1(\Omega)} \|W\|_{V \times H^1(\Omega)} \quad \forall v \in V, \quad Y, W \in V \times H^1(\Omega).$$

If U belongs to $L^2(0, T; V \times H^1(\Omega)) \cap L^\infty(0, T; H \times L^2(\Omega))$ then $b(U, U, \cdot)$ belongs to $L^2(0, T; V^* \times (H^1(\Omega))^*)$ and

$$|b(U, U, \cdot)|_{L^2(0, T; V^* \times (H^1(\Omega))^*)} \leq c |U|_{L^\infty(0, T; H \times L^2(\Omega))} |U|_{L^2(0, T; V \times H^1(\Omega))}.$$

Proof of lemma 6.1. By definition

$$b(U, Y, W) = \int_{\Omega} (v \nabla) y w \, dx + \int_{\Omega} (v \nabla) \tau \kappa \, dx.$$

With Hölders inequality and interpolation inequality, see [15, Lemma 3.3], we get

$$\begin{aligned} b(U, Y, W) &\leq c |v|_{L^4} |\nabla y|_{L^2} |w|_{L^4} + c |v|_{L^4} |\tau|_{H^1} |\kappa|_{L^4} \\ &\leq c |v|_{L^2}^{\frac{1}{2}} |\nabla v|_{L^2}^{\frac{1}{2}} |w|_{L^2}^{\frac{1}{2}} |\nabla w|_{L^2}^{\frac{1}{2}} |\nabla y|_{L^2} + c |v|_{L^2}^{\frac{1}{2}} |\nabla v|_{L^2}^{\frac{1}{2}} |\kappa|_{L^2}^{\frac{1}{2}} |\kappa|_{H^1}^{\frac{1}{2}} |\tau|_{H^1}. \end{aligned}$$

If $U, Y, W \in V \times H^1(\Omega)$, the relation $b(U, Y, W) = -b(U, W, Y)$ gives

$$b(U, Y, W) \leq c |v|_{L^2}^{\frac{1}{2}} |\nabla v|_{L^2}^{\frac{1}{2}} |y|_{L^2}^{\frac{1}{2}} |\nabla y|_{L^2}^{\frac{1}{2}} |\nabla w|_{L^2} + c |v|_{L^2}^{\frac{1}{2}} |\nabla v|_{L^2}^{\frac{1}{2}} |\tau|_{L^2}^{\frac{1}{2}} |\tau|_{H^1}^{\frac{1}{2}} |\kappa|_{H^1}.$$

This implies

$$|b(U, U, Y)| \leq c |U|_{L^2} |U|_{V \times H^1} |Y|_{V \times H^1}.$$

If now $U \in L^2(0, T; V \times H^1(\Omega)) \cap L^\infty(0, T; H \times L^2(\Omega))$, then $b(U(t), U(t), \cdot) \in (V^* \times H^1(\Omega))^*$ for almost every t and the estimate

$$|b(U(t), U(t), \cdot)|_{V^* \times (H^1(\Omega))^*} \leq c |U(t)|_{L^2} |U(t)|_{V \times H^1}$$

implies that $b(U, U, \cdot)$ belongs to $L^2(0, T; V^* \times H^1(\Omega)^*)$. \square

Proof of Theorem 2.1. We begin with proving existence.

- i) We apply the Galerkin procedure. Since $V \times H^1(\Omega)$ is separable and $\mathcal{V} \times \mathcal{C}^\infty(\Omega)$ is dense in $V \times H^1(\Omega)$, there exists a sequence w_1, \dots, w_m, \dots of elements of $\mathcal{V} \times \mathcal{C}^\infty(\Omega)$, which is free and total in $V \times H^1(\Omega)$. For each $m \in \mathbb{N}$ we make the ansatz

$$Y_m = \sum_{i=1}^m g_{im}(t)w_i.$$

for an approximate solution Y_m of (2). Inserting Y_m into (2) and using w_j as test functions we obtain

$$(15) \quad (Y'_m(t), w_j) + a(Y_m(t), w_j) + b(y_m(t), Y_m(t), w_j) + (\gamma g \tau_m(t), w_{j12})_{L^2(\Omega)^2} +$$

$$(16) \quad (\alpha \tau_m(t), w_{j3})_{L^2(\Gamma)} = \langle f(t), w_j \rangle + (\alpha u(t), w_{j3})_{L^2(\Gamma)}, \quad t \in [0, T], \quad j = 1, \dots, m,$$

where Y_{0m} is the orthogonal projection in $H \times L^2(\Omega)$ of Y_0 onto the space spanned by w_1, \dots, w_m . Equations (15),(16) form a nonlinear system of differential equations for the functions g_{1m}, \dots, g_{mm} :

$$\sum_{i=1}^m (w_i, w_j) g'_{im}(t) + \sum_{i=1}^m a(w_i, w_j) g_{im}(t) + \sum_{i,l=1}^m b(w_{i12}, w_l, w_j) g_{im}(t) g_{lm}(t) +$$

$$\sum_{i=1}^m (\gamma g w_{i3}, w_{j12})_{L^2(\Omega)^2} g_{im}(t) + \sum_{i=1}^m (\alpha w_{i3}, w_{j3})_{L^2(\Gamma)} g_{im}(t) = \langle f(t), w_j \rangle + (\alpha u(t), w_{j3})_{L^2(\Gamma)}.$$

Since the mass matrix $(w_i, w_j)_{i,j=1}^m$ is nonsingular this system can be rewritten in the form

$$(17) \quad g'_{im}(t) + \sum_{i=1}^m \alpha_{ij} g_{jm}(t) + \sum_{i,k=1}^m \alpha_{ijk} g_{jm}(t) g_{km}(t) = \sum_{i=1}^m \beta_{ij} \langle f(t), w_j \rangle + \sum_{i=1}^m \tilde{\beta}_{ij} (\alpha u(t), w_{j3})_{L^2(\Gamma)},$$

$$(18) \quad g_{im}(0) = (Y_{0m})_i,$$

with appropriate coefficients $\alpha_{ij}, \alpha_{ijk}, \beta_{ij}, \tilde{\beta}_{ij}$.

System (17),(18) admits a maximal solution defined on some interval $[0, t_m]$. If $t_m < T$, then $|Y_m(T)|$ must tend to $+\infty$ as $t \rightarrow t_m$; the a priori estimates we shall prove in ii) show that this can not happen and therefore $t_m = T$.

- ii) A priori estimates.

We multiply (15) by $g_{jm}(t)$ and add the equations for $j = 1, \dots, m$. This gives

$$(Y'_m(t), Y_m(t)) + a(Y_m(t), Y_m(t)) + b(y_m(t), Y_m(t), Y_m(t)) + (\gamma g \tau_m(t), y_m(t))_{L^2(\Omega)^2}$$

$$+ (\alpha \tau_m(t), \tau_m(t))_{L^2(\Gamma)} = \langle f(t), Y_m(t) \rangle + (\alpha u(t), \tau_m(t))_{L^2(\Gamma)},$$

With [12, Lemma 2.1] and the fact that $\operatorname{div} y_m(t) = 0$ we get

$$b(y_m(t), Y_m(t), Y_m(t)) = 0,$$

and

$$(\gamma g \tau_m(t), y_m(t))_{L^2(\Omega)^2} \geq -c_1 |Y_m(t)|_{H \times L^2(\Omega)}^2.$$

We conclude now

$$\begin{aligned} \frac{d}{dt} |Y_m|^2 + 2a(Y_m(t), Y_m(t)) + 2(\alpha \tau_m(t), \tau_m(t))_{L^2(\Gamma)} \leq \\ 2c_1 |Y_m(t)|_{L^2(\Omega)}^2 + 2 \langle f(t), Y_m(t) \rangle + 2 \langle \alpha u, \tau_m(t) \rangle_{L^2(\Gamma)}, \end{aligned}$$

which implies

$$\begin{aligned} \frac{d}{dt} |Y_m|^2 + 2\nu \|y_m(t)\|^2 + 2a \|\tau_m(t)\|^2 + 2(\alpha \tau_m(t), \tau_m(t))_{L^2(\Gamma)} \leq \\ 2c_1 |Y_m(t)|_{L^2(\Omega)}^2 + 2 \langle u_F, y_m(t) \rangle + 2 \langle u_Q, \tau_m(t) \rangle + 2 \langle \alpha u, \tau_m(t) \rangle_{L^2(\Gamma)}. \end{aligned}$$

Using

$$0 \leq (ca - c^{-1}b)^2 = c^2 a^2 + c^{-2} b^2 - 2ab \quad \forall a, b, c \in \mathbb{R}, c \neq 0$$

we get the estimates

$$(19) \quad 2 \langle u_F, y_m(t) \rangle \leq 2 \|u_F(t)\|_{V^*} \|y_m(t)\|_V \leq \nu \|y_m(t)\|_V^2 + \frac{1}{\nu} \|u_F(t)\|_{V^*}^2,$$

$$(20) \quad 2 \langle u_Q, \tau_m(t) \rangle \leq 2 \|u_Q(t)\|_{(H^1)^*} \|\tau_m(t)\|_{H^1} \leq a \|\tau_m(t)\|_{H^1}^2 + \frac{1}{a} \|u_Q(t)\|_{(H^1)^*}^2,$$

$$(21) \quad 2 \langle \alpha u(t), \tau_m(t) \rangle_{L^2(\Gamma)} \leq 2 \|\alpha u(t)\| \|\tau_m(t)\| \leq \alpha \|\tau_m(t)\|_{L^2(\Gamma)}^2 + \frac{1}{\alpha} \|\alpha u(t)\|_{L^2(\Gamma)}^2,$$

and thus,

$$\begin{aligned} \frac{d}{dt} |Y_m(t)|^2 + \nu \|y_m(t)\|^2 + a \|\tau_m(t)\|^2 + \alpha \|\tau_m(t)\|_{L^2(\Gamma)}^2 \leq \\ 2c_1 |Y_m(t)|_{L^2(\Omega)}^2 + \frac{1}{\nu} \|u_F(t)\|_{V^*}^2 + \frac{1}{a} \|u_Q(t)\|_{(H^1)^*}^2 + \|u(t)\|_{L^2(\Gamma)}^2, \end{aligned}$$

as well as

$$(22) \quad \frac{d}{dt} |Y_m(t)|^2 \leq 2c_1 |Y_m(t)|_{L^2(\Omega)}^2 + \frac{1}{\nu} \|u_F(t)\|_{V^*}^2 + \frac{1}{a} \|u_Q(t)\|_{(H^1)^*}^2 + \|u(t)\|_{L^2(\Gamma)}^2.$$

Integrating (22) from 0 to s we obtain

$$\begin{aligned} |Y_m(s)|^2 \leq |Y_m(0)|^2 + 2c_1 \int_0^s |Y_m(t)|_{L^2(\Omega)}^2 dt + \\ + \frac{1}{\nu} \int_0^s \|u_F(t)\|_{V^*}^2 dt + \frac{1}{a} \int_0^s \|u_Q(t)\|_{(H^1)^*}^2 dt + \int_0^s \|u(t)\|_{L^2(\Gamma)}^2 dt. \end{aligned}$$

Gronwall's Lemma then yields:

$$|Y_m(s)|^2 \leq (|Y_m(0)|^2 + \frac{1}{\nu} \int_0^s \|u_F(t)\|_{V^*}^2 dt + \frac{1}{a} \int_0^s \|u_Q(t)\|_{(H^1)^*}^2 dt + \int_0^s \|u(t)\|^2 dt) e^{2c_1 s},$$

$$\begin{aligned} |Y_m(s)|^2 &\leq (|Y_m(0)|^2 + \frac{1}{\nu} \int_0^T \|u_F(t)\|_{V^*}^2 dt + \\ &+ \frac{1}{a} \int_0^T \|u_Q(t)\|_{(H^1)^*}^2 dt + \int_0^T \|u(t)\|^2 dt) e^{2c_1 T} \quad \forall s \in [0, T]. \end{aligned}$$

Hence,

$$\begin{aligned} \sup_{s \in [0, T]} |Y_m(s)|^2 &\leq (|Y_m(0)|^2 + \frac{1}{\nu} \int_0^T \|u_F(t)\|_{V^*}^2 dt + \\ &+ \frac{1}{a} \int_0^T \|u_Q(t)\|_{(H^1)^*}^2 dt + \int_0^T \|u(t)\|^2 dt) e^{2c_1 T}, \end{aligned}$$

which implies that the sequence $\{Y_m\}_m$ remains in a bounded set of $L^\infty(0, T; H \times L^2(\Omega))$. Since $c_2 \|\tau\|_{H^1(\Omega)} \leq \|\tau\|_{H_0^1(\Omega)} + \|\tau\|_{L^2(\Gamma)}$ for some $c_2 > 0$ we get

$$c_3 \|Y_m(t)\|_{H^1(\Omega)} \leq \nu \|y_m(t)\|_V^2 + a \|\tau_m(t)\|_{H_0^1(\Omega)}^2 + \alpha \|\tau_m(t)\|_{L^2(\Gamma)}^2.$$

From (22) we now deduce

$$(23) \quad \frac{d}{dt} |Y_m(t)|^2 + c_3 \|Y_m(t)\|_{H^1(\Omega)} \leq 2c_1 |Y_m(t)|_{L^2(\Omega)}^2 + \frac{1}{\nu} \|u_F(t)\|_{V^*}^2 + \frac{1}{a} \|u_Q(t)\|_{(H^1)^*}^2 + \|u(t)\|^2.$$

Now we integrate (23) from 0 to T and apply Gronwall's Lemma once more to obtain the estimate

$$\begin{aligned} |Y_m(T)|^2 + c_3 \int_0^T \|Y_m(t)\|_{H^1(\Omega)} dt &\leq (|Y_m(0)|^2 + \frac{1}{\nu} \int_0^T \|u_F(t)\|_{V^*}^2 dt + \\ &+ \frac{1}{a} \int_0^T \|u_Q(t)\|_{(H^1)^*}^2 dt + \int_0^T \|u(t)\|^2 dt) \exp(2c_1 T). \end{aligned}$$

This implies that the sequence $\{Y_m\}_m$ remains in a bounded set of $L^2(0, T; V \times H^1(\Omega))$.

It is now straightforward to conclude that a subsequence $Y_{m'}$ exists such that $Y_{m'} \rightarrow Y$ in $L^2(0, T, V \times H^1(\Omega))$ weakly, and in $L^\infty(0, T, H \times L^2(\Omega))$ weak-star.

iii) Now we will show that $Y_{m'} \rightarrow Y$ in $L^2(0, T, H \times L^2(\Omega))$ strongly.

For this purpose we firstly show that $\{\frac{d}{dt} Y_m\} \subset L^{4/3}(V^* \times (H^1(\Omega))^*)$, see Constantin and [3]. First let us consider (15). Since $\{Y_m\}_m$ is bounded in $L^2(0, T; V \times H^1(\Omega))$ it

follows that $a(Y_m, \cdot)$ is bounded in $L^2(0, T; V^* \times (H^1(\Omega))^*)$. This also holds for the forms $(\gamma g \tau_m, \cdot)_{L^2(\Omega)^2} + (a \tau_m, \cdot)_{L^2(\Gamma)}$. Note that $Y_m = (y_m, \tau_m)^T$. By assumption f is bounded in $L^2(0, T; V^* \times (H^1(\Omega))^*)$.

It remains to investigate the term $b(y_m, Y_m, \cdot)$.

Using

$$\begin{aligned} \|v\|_{L^4(\Omega)} &\leq \|\nabla v\|_{L^2(\Omega)} \leq \|v\|_{V \times H^1(\Omega)}, \\ \|y_m\|_{L^4(\Omega)} &\leq c \|y_m\|_{L^2(\Omega)}^{\frac{1}{2}} \|\nabla y_m\|_{L^2(\Omega)}^{\frac{1}{2}}, \\ \|\tau_m\|_{L^4(\Omega)} &\leq c \|\tau_m\|_{L^2(\Omega)}^{\frac{1}{2}} \|\tau_m\|_{H^1(\Omega)}^{\frac{1}{2}}, \end{aligned}$$

and the Hölder-inequality we get

$$\begin{aligned} &\int_{\Omega} (y_m \nabla) Y_m v dx = \int_{\Omega} (y_m \nabla) y_m v_y dx + \int_{\Omega} (y_m \nabla) \tau_m v_{\tau} dx \\ &\leq c_1 \|y_m\|_{L^4(\Omega)} \|\nabla y_m\|_{L^2(\Omega)} \|v_y\|_{L^4(\Omega)} + c_2 \|y_m\|_{L^4(\Omega)} \|\tau_m\|_{H^1(\Omega)} \|v_{\tau}\|_{L^4(\Omega)} \\ &\leq c_3 \|y_m\|_{L^2(\Omega)}^{\frac{1}{2}} \|\nabla y_m\|_{L^2(\Omega)}^{\frac{1}{2}} (\|\nabla y_m\|_{L^2(\Omega)} \|v_y\|_V + \|\tau_m\|_{H^1(\Omega)} \|v_{\tau}\|_{H^1(\Omega)}) \\ &\leq c_3 \|y_m\|_{L^2(\Omega)}^{\frac{1}{2}} \|\nabla y_m\|_{L^2(\Omega)}^{\frac{1}{2}} (\|\nabla y_m\|_{L^2(\Omega)} + \|\tau_m\|_{H^1(\Omega)}) \|v\|_{V \times H^1(\Omega)}, \end{aligned}$$

so that

$$\begin{aligned} &\int_0^T \|b(y_m, Y_m, \cdot)\|_{V^* \times (H^1(\Omega))^*}^{\frac{4}{3}} dt \\ &\leq c_4 \int_0^T \|y_m\|_{L^2(\Omega)}^{\frac{2}{3}} (\|\nabla y_m\|_{L^2(\Omega)}^{\frac{3}{2}} + \|\nabla y_m\|_{L^2(\Omega)}^{\frac{1}{2}} \|\tau_m\|_{H^1(\Omega)})^{\frac{4}{3}} dt \\ &\leq 2c_4 \int_0^T \|y_m\|_{L^2(\Omega)}^{\frac{2}{3}} \max(\|\nabla y_m\|_{L^2(\Omega)}^2, \|\nabla y_m\|_{L^2(\Omega)}^{\frac{2}{3}} \|\tau_m\|_{H^1(\Omega)}^{\frac{4}{3}}) dt. \end{aligned}$$

Since $\|Y_m(t)\|_{L^2(\Omega)}$ is bounded uniformly, the right argument of the max-function can be estimated as

$$\int_0^T \|\nabla y_m\|_{L^2(\Omega)}^{\frac{2}{3}} \|\tau_m\|_{H^1(\Omega)}^{\frac{4}{3}} dt \leq \left(\int_0^T \|\nabla y_m\|_{L^2(\Omega)}^2 dt \right)^{\frac{1}{3}} \left(\int_0^T \|\tau_m\|_{H^1(\Omega)}^2 dt \right)^{\frac{2}{3}},$$

and since $\|\nabla y_m(t)\|_{L^2(\Omega)}^2$ and $\|\tau_m(t)\|_{H^1(\Omega)}^2$ are uniformly integrable with respect to m , we have $\left\{ \frac{d}{dt} Y_m \right\} \subset L^{4/3}(V^* \times (H^1(\Omega))^*)$. Together with $\{Y_m\} \subset L^2(0, T; V \times H^1(\Omega))$ from ii) it follows that $\{Y_m\} \subset W_{4/3}^2(0, T; V \times H^1(\Omega))$ is bounded.

By the Aubin-Dubinskii-Lemma, see [3], $W_{4/3}^2(0, T; V \times H^1(\Omega))$ compactly embeds into $L^2(0, T; H \times L^2(\Omega))$. Therefor $Y_{m'} \rightarrow Y$ in $L^2(0, T, H \times L^2(\Omega))$ strongly for a subsequence.

iv) This convergence results enable us to pass to the limit in (15)-(16). Let ψ be a continuously differentiable function on $[0, T]$ with $\psi(T) = 0$. We multiply (15) by $\psi(t)$, and integrate by parts. This leads to

$$\begin{aligned}
& - \int_0^T (Y_m(t), \psi'(t)w_j)dt + \int_0^T a(Y_m(t), w_j\psi(t))dt + \int_0^T b(y_m(t), Y_m(t), w_j\psi(t))dt + \\
(24) \quad & + \int_0^T (\gamma g\tau_m(t), w_{j_{12}}\psi(t))_{L^2(\Omega)^2}dt + \int_0^T (\alpha\tau_m(t), w_{j_3}\psi(t))_{L^2(\Gamma)}dt \\
& = \int_0^T \langle f(t), w_j\psi(t) \rangle dt + \int_0^T (\alpha u(t), w_{j_3}\psi(t))_{L^2(\Gamma)}dt + (Y_{0m}, w_j)\psi(0).
\end{aligned}$$

Passing to the limit with the sequence m' is easy for the linear terms; for the non-linear term we apply [15, Lemma 3.2] and obtain for every vector function w with components in $C^1((0, T) \times \Omega)$

$$\int_0^T b(y_\mu(t), Y_\mu(t), w(t))dt \rightarrow \int_0^T b(y(t), Y(t), w(t))dt \quad (\mu \rightarrow \infty).$$

In the limit we find that the equation

$$\begin{aligned}
& - \int_0^T (Y(t), \psi'(t)U)dt + \int_0^T a(Y(t), U\psi(t))dt + \int_0^T b(y(t), Y(t), U\psi(t))dt + \\
(25) \quad & + \int_0^T (\gamma g\tau(t), v\psi(t))_{L^2(\Omega)^2}dt + \int_0^T (\alpha\tau(t), w\psi(t))_{L^2(\Gamma)}dt \\
& = \int_0^T \langle f(t), U\psi(t) \rangle dt + \int_0^T (\alpha u(t), w\psi(t))_{L^2(\Gamma)}dt + (Y_0, U)\psi(0),
\end{aligned}$$

holds for $U = (v, w)^T$ in the set $\{w_1, w_2, \dots\}$; by linearity this equation holds for U equal to any finite linear combination of the w_j , and by a continuity argument (25) is still valid for any $U \in V \times H^1(\Omega)$. Thus, Y satisfies (2) in the distributional sense.

Finally, it remains to prove that Y satisfies the initial condition (3). To show this we multiply (2) by ψ , and integrate. Integrating the first term by parts, gives

$$\begin{aligned}
& - \int_0^T (Y(t), \psi'(t)U)dt + \int_0^T a(Y(t), U\psi(t))dt + \int_0^T b(y(t), Y(t), U\psi(t))dt + \\
(26) \quad & + \int_0^T (\gamma g\tau(t), v\psi(t))_{L^2(\Omega)^2}dt + \int_0^T (\alpha\tau(t), w\psi(t))_{L^2(\Gamma)}dt \\
& = \int_0^T \langle f(t), U\psi(t) \rangle dt + \int_0^T (\alpha u(t), w\psi(t))_{L^2(\Gamma)}dt + (Y(0), U)\psi(0),
\end{aligned}$$

By comparison with (25),

$$(Y(0) - Y_0, U)\psi(0) = 0.$$

Now we choose ψ with $\psi(0) = 1$; thus

$$(Y(0) - Y_0, U) = 0. \quad \forall U \in V \times H_1(\Omega),$$

and (3) follows.

Uniqueness:

- i) We first note that $b(U, U, \cdot)$ belongs to $L^2(0, T; V^* \times H^1(\Omega)^*)$, see Lemma 6.1, which implies that Y' also belongs to $L^2(0, T; V^* \times H^1(\Omega)^*)$.

This enables us to apply [15, Lemma 1.2 in Ch. III §3], which claims that Y is almost everywhere equal to a continuous function. Thus

$$Y \in \mathcal{C}([0, T]; H \times L^2(\Omega)),$$

and (4) follows immediately. The same lemma asserts that for any function Y in $L^2(0, T; V \times H^1(\Omega))$ which satisfies $Y' \in L^2(0, T; V^* \times (H^1(\Omega))^*)$, the equation

$$(27) \quad \frac{d}{dt} |Y(t)|^2 = 2 \langle Y'(t), Y(t) \rangle$$

is valid, which will be used below.

- ii) Proof of uniqueness. Let us assume that Y_1 and Y_2 are two solutions of (2)-(3), and let $Y = Y_1 - Y_2$. As shown before Y_1, Y_2 , and thus Y are in $L^2(0, T; V^* \times (H^1(\Omega))^*)$.

The difference $Y = Y_1 - Y_2$ satisfies

$$(28) \quad \frac{d}{dt}(Y, U) + a(Y, U) + (\gamma g \tau, v)_{L^2(\Omega)^2} + (\alpha \tau, \eta)_{L^2(\Gamma)} = b(y_2, Y_2, U) - b(y_1, Y_1, U)$$

$$\forall U \in V \times H^1(\Omega), \text{ and almost all } t \in (0, T),$$

$$(29) \quad Y(0) = 0.$$

Taking $U = Y(t)$ and using (27), we get

$$\begin{aligned} \frac{d}{dt} |Y(t)|^2 + 2\nu \|y(t)\|^2 + 2a \|\tau(t)\|^2 + 2\alpha |\tau(t)|_{L^2(\Gamma)}^2 + 2 \langle \gamma g \tau(t), y(t) \rangle \\ = 2b(y_2(t), Y_2(t), Y(t)) - 2b(y_1(t), Y_1(t), Y(t)). \end{aligned}$$

Since $b(v, W, W) = 0 \quad \forall v \in V, W \in H_0^1(\Omega)^2 \times H^1(\Omega)$, the right-hand side is equal to

$$-2b(y(t), Y_2(t), Y(t)).$$

From Lemma 6.1 we deduce

$$\begin{aligned} |-2b(y(t), Y_2(t), Y(t))| &\leq c |y|_{L^2}^{\frac{1}{2}} |\nabla y|_{L^2}^{\frac{1}{2}} |y|_{L^2}^{\frac{1}{2}} |\nabla y|_{L^2}^{\frac{1}{2}} |\nabla y_2|_{L^2} + c |y|_{L^2}^{\frac{1}{2}} |\nabla y|_{L^2}^{\frac{1}{2}} |\tau|_{L^2}^{\frac{1}{2}} |\tau|_{H^1}^{\frac{1}{2}} |\tau_2|_{H^1} \\ &\leq c |y|_{L^2} |\nabla y_2|_{L^2} |Y|_{V \times H^1(\Omega)} + c |y|_{L^2} |\tau_2|_{H^1} |Y|_{V \times H^1(\Omega)} \\ &\leq c |Y|_{L^2} |Y_2|_{V \times H^1(\Omega)} |Y|_{V \times H^1(\Omega)}. \end{aligned}$$

Using Young's inequality we estimate further

$$c|Y|_{L^2} |Y_2|_{V \times H^1(\Omega)} |Y|_{V \times H^1(\Omega)} \leq 2 \min(\nu, a) |Y|_{V \times H^1(\Omega)}^2 + \frac{1}{\epsilon} (c|Y|_{L^2} |Y_2|_{V \times H^1(\Omega)})^2.$$

The term

$$|2 \langle \gamma g \tau(t), y(t) \rangle| \leq 2\gamma |g| |Y|_{L^2(\Omega)}^2$$

is also majorized. We can conclude

$$\frac{d}{dt} |Y(t)|^2 \leq \left(\frac{c^2}{\epsilon} |Y_2|_{V \times H^1(\Omega)}^2 + 2\gamma |g|\right) |Y(t)|_{L^2(\Omega)}^2 \quad \forall t \in [0, T],$$

so that

$$\frac{d}{dt} |Y(t)|^2 \leq c(\nu, a, \gamma g, Y_2(t), t) |Y(t)|_{L^2(\Omega)}^2 \quad \forall t \in [0, T].$$

Integrating from 0 to s and using (29) gives

$$|Y(s)|^2 \leq \int_0^s c(\nu, a, \gamma g, Y_2(t), t) |Y(t)|^2 dt$$

Finally Gronwall's-Lemma implies

$$|Y(s)|^2 \leq 0 \quad \forall s \in [0, T],$$

which gives

$$Y_1 = Y_2,$$

so that the solution of (1) is unique.

□

Acknowledgement

The authors acknowledge support of the Collaborative Reserach Grant SFB 609 *Elektromagnetische Strömungsbeeinflussung in Metallurgie, Kristallzüchtung und Elektrochemie*, sponsored by the Deutsche Forschungsgemeinschaft

References

- [1] F. Abergel & R. Temam: *On Some Control Problem in Fluid Mechanics*. Theoretical and Computational Fluid Dynamics, 303-325, Springer, 1990.
- [2] H. Choi, M. Hinze & K. Kunisch: *Instantaneous Control of Backward-Facing Step Flows*. Applied Numerical Mathematics 31, 133-158 (1999), see also Preprint No. 571/97, Technische Universität Berlin

- [3] P. Constantin & C. Foias: *Navier-Stokes Equations*. Chicago Lectures in Mathematics, The University of Chicago Press 1988.
- [4] R. Glowinski: *Finite element methods for the numerical simulation of incompressible viscous flow; Introduction to the control of the Navier-Stokes equations*. Lectures in Applied Mathematics, 28, 1991.
- [5] M. D. Gunzburger: *Perspectives in Flow Control and Optimization*. SIAM, 2003.
- [6] M. Hinze: *Optimal and instantaneous control of the instationary Navier-Stokes equations*. Habilitationsschrift, 2000. Fachbereich Mathematik, Technische Universität Berlin.
- [7] M. Hinze: *Instantaneous closed loop control of the Navier-Stokes system*. Preprint, to appear in SICON.
- [8] M. Hinze & K. Kunisch: *Control strategies for fluid flows - optimal versus suboptimal control*. ENUMATH 97, Eds. H.G. Bock et al., World Scientific, Singapore, 351-358 (1997), see also Preprint No. 573/98, Technische Universität Berlin
- [9] M. Hinze & S. Volkwein: *Instantaneous control for the instationary Burgers equation - convergence analysis & numerical implementation*. Nonlinear Analysis T.M.A. 50, 1-26 (2002), see also Bericht Nr. 170 des Spezialforschungsbereichs F003 Optimierung und Kontrolle, Karl-Franzens Universität Graz
- [10] M. Hinze & D. Wachsmuth: *Fast closed loop control of the Navier-Stokes system*. Preprint MATH-NM-08-2003, Institut für Numerische Mathematik, Technische Universität Dresden (2003), submitted
- [11] K. Kunisch & X. Marduel: *Optimal control of non-isothermal viscoelastic fluid flow*. J. Non-Newtonian Fluid Mech. 88, No.3, 261-301 (2000).
- [12] H.-C. Lee & O. Yu. Imanuvilov: *Analysis of Neumann Boundary optimal Control problems for the stationary Boussinesq equations including solid media*. SIAM J. Control Optim. Vol. 39, No.2, pp. 457-477 2000.
- [13] X. Marduel & K. Kunisch: *Suboptimal Control of Transient Non-Isothermal Viscoelastic Fluid Flow*. Preprint, Special Research Center for Optimization and Control, University of Graz, (1999).
- [14] U. Matthes: *Instantane Kontrolle der Boussinesq Approximation*. Diplomarbeit, 2003. Fachrichtung Mathematik, Technische Universität Dresden.
- [15] R. Temam: *Navier-Stokes Equations, Theory and Numerical Analysis*. North-Holland 1984.
- [16] D. Wachsmuth: *Numerische Analysis eines Verfahrens der Momentansteuerung*. Diplomarbeit, 2002. Fakultät für Mathematik, Technische Universität Chemnitz.